DOI: 10.1093/jnci/djr029
Advance Access publication on February 17, 2011.

ARTICLE

Chemopreventative Potential of the Cruciferous Vegetable Constituent Phenethyl Isothiocyanate in a Mouse Model of Prostate Cancer

Anna A. Powolny, Ajay Bommareddy, Eun-Ryeong Hahm, Daniel P. Normolle, Jan H. Beumer, Joel B. Nelson, Shivendra V. Singh

Manuscript received May 27, 2010; revised January 10, 2011; accepted January 12, 2011.

Correspondence to: Shivendra V. Singh, PhD, Department of Pharmacology and Chemical Biology, University of Pittsburgh School of Medicine, 2.32A Hillman Cancer Center Research Pavilion, 5117 Centre Ave, Pittsburgh, PA 15213 (e-mail: singhs@upmc.edu).

Background This study was undertaken to determine the chemopreventative efficacy of phenethyl isothiocyanate (PEITC), a bioactive constituent of many edible cruciferous vegetables, in a mouse model of prostate cancer, and to identify potential biomarker(s) associated with PEITC response.

Methods The chemopreventative activity of dietary PEITC was investigated in Transgenic Adenocarcinoma of Mouse Prostate mice that were fed a control diet or one containing 3 μmol PEITC/g (n = 21 mice per group) for 19 weeks. Dorsolateral prostate tissue sections were stained with hematoxylin and eosin for histopathologic evaluations and subjected to immunohistochemistry for analysis of cell proliferation (Ki-67 expression), autophagy (p62 and LC3 protein expression), and E-cadherin expression. Autophagosomes were visualized by transmission electron microscopy. Apoptotic bodies were detected by terminal deoxynucleotidyl transferase–mediated dUTP nick-end labeling. Plasma proteomics was performed by two-dimensional gel electrophoresis followed by mass spectrometry to identify potential biomarkers of PEITC activity. All statistical tests were two-sided.

Results Administration of PEITC (3 μmol/g diet) decreased incidence (PEITC diet vs control diet, mean = 21.65 vs 57.58%, difference = −35.93%, 95% confidence interval = −45.48% to −13.10%, $P = .04$) as well as burden (affected area) (PEITC diet vs control diet, mean = 18.53% vs 45.01%, difference = −26.48%, 95% confidence interval = −49.78% to −3.19%, $P = .02$) of poorly differentiated tumors in the dorsolateral prostate of transgenic mice compared with control mice, with no toxic effects. PEITC-mediated inhibition of prostate carcinogenesis was associated with induction of autophagy and overexpression of E-cadherin in the dorsolateral prostate. However, PEITC treatment was not associated with a decrease in cellular proliferation, apoptosis induction, or inhibition of neoangiogenesis. Plasma proteomics revealed distinct changes in the expression of several proteins (eg, suppression of clusterin protein) in the PEITC-treated mice compared with control mice.

Conclusions In this transgenic model, dietary PEITC suppressed prostate cancer progression by induction of autophagic cell death. Potential biomarkers to assess the response to PEITC treatment in plasma were identified.

J Natl Cancer Inst 2011;103:571–584

Despite improvements in screening efforts and the continuous evolution of targeted therapies, prostate cancer continues to be a leading cause of cancer-related deaths in American men (1). Because many of the risk factors associated with prostate carcinogenesis (eg, age and genetic predisposition) are not easily adjustable, novel strategies for prevention of this disease are necessary to reduce morbidity and mortality.

The active constitutive agents in natural products are frequently investigated for their potential cancer preventative and therapeutic properties (2–6). Epidemiological studies support an inverse association between the intake of certain fruits and vegetables, including cruciferous vegetables, and the risk of many cancers, including cancer of the prostate (7–10). The anticarcinogenic effects of cruciferous vegetables have been attributed to chemicals with an isothiocyanate (–N=C=S) functional group (11,12). Isothiocyanates are generated through myrosinase-mediated hydrolysis of corresponding glucosinolates (11,12). Phenethyl isothiocyanate (PEITC) has demonstrated chemopreventative efficacy in vivo in chemically induced cancer and a favorable safety profile in preclinical animal models (13–18).

Recent studies, including those from our laboratory, have revealed that PEITC suppresses the growth of cancer cells both in vitro and in vivo (19–24). The mechanisms behind the anticancer effects of PEITC are not fully understood. However, several cellular responses to this potential cancer chemopreventative agent have been previously described (19–26), including apoptosis mediated by both c-Jun amino terminal kinase and extracellular signal-regulated kinase (19,20), G_2/M phase cell cycle arrest

CONTEXT AND CAVEATS

Prior knowledge

Prior studies have shown that phenethyl isothiocyanate (PEITC), a bioactive constituent of many edible cruciferous vegetables, has antitumor effects in human cancer cells in vitro and in vivo. However, the exact mechanisms of PEITC treatment in vivo are not fully understood.

Study design

Transgenic Adenocarcinoma of Mouse Prostate mice were fed a control diet or a diet supplemented with PEITC. Toxicity as well as tumor incidence and burden were measured. Potential plasma biomarkers of PEITC treatment were also investigated.

Contribution

No toxic effects were observed in mice fed a PEITC diet. Tumor incidence and burden in prostates were statistically significantly reduced in PEITC-treated mice compared to mice fed the control diet and were associated with increased markers of autophagy and migration. Also, clusterin was identified as a potential plasma biomarker of PEITC-induced chemopreventative activity.

Implications

PEITC is a potential chemopreventative agent for prostate cancer. Clusterin levels in patient plasma may be associated with PEITC activity and its function as a potential biomarker should be investigated in future studies.

Limitations

Previous reports of decreased proliferation and angiogenesis, and increased apoptosis in human cell lines was not confirmed. Furthermore, it is unknown if dietary administration of PEITC would be adequate in humans or if pharmacological PEITC would be necessary to achieve chemopreventative activity.

From the Editors

(21), suppression of nuclear factor-κB-regulated gene expression (22), and Atg5-mediated autophagy (25). We have also previously shown that PEITC treatment by oral gavage of male athymic mice carrying subcutaneously implanted PC-3 human prostate tumors resulted in inhibition of tumor growth (24). Furthermore, PEITC treatment inhibits angiogenesis (capillary-like tube structure formation) and migration of human umbilical vein endothelial cells and PC-3 prostate cancer cell migration in vitro by suppressing the activity of the Akt serine threonine kinase (27). The PEITC-mediated inhibition of angiogenesis is also evident in an ex vivo model with a chicken egg chorioallantoic assay (27).

Although cellular studies constitute an important step in the development of chemopreventative drugs by providing mechanistic insights, demonstrating preventative efficacy in animal models and validating cellular observations in vivo are necessary for the rational design of clinical trials to investigate potential cancer protective agents. The goals of our study were to determine if dietary administration of PEITC is protective against prostate cancer development in a transgenic mouse model (Transgenic Adenocarcinoma of Mouse Prostate [TRAMP]), elucidate the anti cancer mechanisms of PEITC in vivo, and identify biomarker(s) with predictive value for PEITC response for use in future clinical applications as biological surrogates.

Materials and Methods

Reagents

PEITC (~98% purity), benzyl isothiocyanate (~98% purity), diallyl trisulfide (~98% purity), and D,L-sulforaphane (~98% purity) were purchased from LKT Laboratories (St Paul, MN). Allyl isothiocyanate (95% purity) and reagent grade gluconasturtiin were obtained from Sigma-Aldrich (St Louis, MO) and Chromadex (Irvine, CA), respectively. AIN-76A (control) diet and PEITC-supplemented AIN-76A diet (referred to as PEITC-supplemented diet) were custom prepared by Harlan-Teklad (Indianapolis, IN). Mouse monoclonal anti–T antigen antibody (PAb101, 1:200 dilution) was from BD Pharmingen (San Diego, CA). Polyclonal goat anti–CD31 (also known as platelet/endothelial cell adhesion molecule 1; M-20, 1:750 dilution), polyclonal goat anti–clusterin (C-18, 1:200 dilution), polyclonal rabbit anti–microtubule-associated protein 1 light chain 3 (LC3; H-50, 1:100 dilution), and mouse monoclonal anti–p62 (D-3, 1:75 dilution) antibodies were purchased from Santa Cruz Biotechnology (Santa Cruz, CA). Mouse monoclonal anti–E-cadherin antibody (36/E-cadherin, 1:2000 dilution) was purchased from BD Transduction Laboratories (San Diego, CA). Rat monoclonal anti–Ki-67 antibody (TEC-3, 1:50 dilution) was purchased from DakoCytomation (Carpinteria, CA). Cell culture reagents including media, serum, and antibiotics were purchased from Invitrogen-Life Technologies (Carlsbad, CA).

Mouse Models and PEITC Treatments

Six- to eight-week-old female TRAMP mice in C57BL/6 background and male FVB mice were purchased from Jackson Laboratories (Bar Harbor, ME). Use of mice and their care for the study were in accordance with the University of Pittsburgh Institutional Animal Care and Use Committee guidelines. Mice in this study were maintained in a climate controlled environment with a 12-hour light/12-hour dark cycle and both food and water were available ad libitum.

The TRAMP model was selected for these studies because of the following: 1) a well-defined course of disease progression with resemblance to human prostate cancer development from prostatic intraepithelial neoplasia (PIN) to well-differentiated (WD) and poorly differentiated (PD) carcinoma and distant site metastasis (28,29), 2) studies can be completed in 6–7 months (28–31), and 3) the TRAMP model has been used successfully to test the chemopreventative efficacy of several natural agents (30,31). Male transgenic [C57BL/6 X FVB] F1 TRAMP mice and age-matched wild-type (nontransgenic) littermates were obtained by crossing TRAMP females in the C57BL/6 background with male FVB mice. Transgene verification was performed as described by Greenberg et al. (28).

In the first experiment, 5-week-old wild-type male C57BL/6 mice were given either a control diet (n = 6) or a diet supplemented with 3 μmol PEITC/g (n = 6). In the second experiment, 5-week-old male TRAMP mice were randomized into the following groups: TRAMP-control diet (n = 25), TRAMP-1.5 μmol PEITC/g diet (n = 20), and TRAMP-3 μmol PEITC/g diet

(n = 25). Four mice from the TRAMP-control diet group, one mouse from the TRAMP-1.5 μmol PEITC/g diet group, and four mice from the TRAMP-3 μmol PEITC/g diet group were removed from the study because of premature development of large tumors in the prostate or other organs (eg, kidney) or because of death caused by a congenital defect. Body weights and diet consumptions were recorded once each week in both experiments. Sample size for the first experiment (wild-type nontransgenic littermates) was not made on the basis of a power calculation because the primary objective of this study was to determine the safety and bioavailability of PEITC. The power of the chemopreventative efficacy experiment was 80% if the difference in histological burden between PEITC arms was 27% or greater.

After 19 weeks of feeding, plasma was collected for further analysis and the mice were killed by CO_2 inhalation followed by cervical dislocation. Wet weights of all vital organs, the urogenital tract, and the prostate were recorded. Dorsolateral prostate tissues from TRAMP mice receiving the control diet (n = 2) or the PEITC-supplemented diet (3 μmol PEITC/g, n = 3) were used for electron microscopy and thus were not available for histopathologic evaluation. Dorsolateral prostate tissues from the mice fed control and PEITC-supplemented diets were placed in 10% neutral buffered formalin and paraffin embedded. Tissues were sectioned at 4–5 μm thickness for hematoxylin and eosin (H&E) staining, terminal deoxynucleotidyl transferase–mediated dUTP nick-end labeling (TUNEL) assay, and immunohistochemical analysis of T antigen, Ki-67, CD31, p62, LC3, and E-cadherin.

Pathological Evaluation of Prostate Tissues

H&E-stained sections of the dorsolateral prostate from wild-type (nontransgenic littermates) and TRAMP mice treated as described above were blindly examined by two observers. Ten randomly selected, non-overlapping, non-necrotic fields were used to evaluate the incidence and burden (affected area) of prostate cancer pathologies. Pathological grading was consistent with the criteria defined by previous studies (28–31). Briefly, normal prostate was characterized by open ducts lined with epithelial cells surrounded by a thin sheet of smooth muscle cells. PIN was characterized by the piling up of the epithelial cells, changes in the nuclear to cytoplasmic ratio, elongation of the nucleus, and epithelial stratification and formation of cribriform structures (high-grade PIN). WD exhibited clear invasion of the epithelial cells into the stroma, whereas PD was characterized by sheets of anaplastic cells with little or no glandular structures.

Determination of PEITC Levels in Plasma and Prostate

PEITC concentrations in the plasma and prostates of wild-type (nontransgenic) mice fed a control diet (n = 3) or a diet supplemented with 3 μmol PEITC/g (n = 3) were determined according to the method described for rat plasma (32) with some modifications. Our assay extends the range to 6–10 000 nM, reduces the sample volume to 0.2 mL, simplifies the extraction procedure, and reduces derivatization time. Briefly, 5 μL of 2 μg/mL [D_5]-PEITC (internal standard purchased from C/D/N ISOTOPES INC, Quebec, Canada) was added to 0.2 mL plasma or added to 0.2 mL 1:4 (wt/vol) tissue homogenate in phosphate-buffered saline (PBS) (1.5 mM potassium phosphate, 15.2 mM sodium phosphate dibasic, 137 mM sodium chloride, and 2.7 mM potassium chloride, at pH 7.4) and extracted with 0.8 mL hexane. Hexane was decanted and PEITC was derivatized with 1 mL of 2 M ammonia in isopropanol at 50°C for 1 hour. Dried residues were reconstituted in 50 μL of mobile phase, and an aliquot (25 μL) was subjected to high performance liquid chromatography consisting of an Agilent 1100 autosampler, a binary pump, and a Phenomenex Synergi-Hydro RP (4 μm, 100 × 2 mm) column (Phenomenex, Torrance, CA). The mobile phase consisted of acetonitrile/water (50:50 vol/vol) with 0.1% formic acid at 0.2 mL/min. Analytes were detected with a Quattromicro quadruple mass spectrometer (Waters, Milford, MA) with electrospray ionization in positive-ion mode, monitoring *m/z* 181.2–105.0 for PEITC, and *m/z* 186.2–110.0 for [D_5]-PEITC. PEITC was eluted at a retention time of 2.4 minutes. PEITC was quantified by calculating the PEITC:internal standard ratio and back-calculating unknown samples with a concomitantly analyzed standard curve in control plasma or prostate homogenate. Standard curves were linear over the range of 6–10 000 nM and displayed acceptable performance (accuracy of at least 14 of 16 calibrators was within 15% of the nominal concentrations; and more than four of six plasma quality controls at 18, 200, and 8000 nM were within 15% of the nominal concentrations).

Immunohistochemistry

Immunohistochemistry was performed as previously described (30,31). Briefly, dorsolateral prostate sections were quenched with 3% hydrogen peroxide and blocked with normal serum. The sections were then probed with the desired primary antibody (anti–Ki-67, anti–T antigen, anti–p62, anti–LC3, anti–CD31, or anti–E-cadherin), washed with Tris-buffered saline (25 mM Tris containing 150 mM NaCl and 2 mM KCl, at pH 7.4), and incubated with an appropriate secondary antibody. The characteristic brown color was developed by incubation with 3,3′-diaminobenzidine. The sections were counterstained with Meyers Hematoxylin (Sigma-Aldrich) and examined under a Leica microscope (Leica Microsystems, Bannockburn, IL). The images were captured and analyzed with Image ProPlus 5.0 software (Media Cybernetics, Bethesda, MD) as previously described (30,31). At least five non-overlapping, non-necrotic images were captured from dorsolateral prostate sections from mice fed control diet and PEITC-supplemented diet and analyzed with the Red–Green–Blue color histogram tool from Image ProPlus 5.0 software. The pixel intensity for brown color from the 3,3′-diaminobenzidine stain was determined for tabulation of percent area. Because of variation in pixel intensity for different immunohistochemical stains, a universal cutoff was not feasible.

TUNEL Assay

Dorsolateral prostate sections from the TRAMP mice on control diet (n = 19) or 3 μmol PEITC/g diet (n = 18) were deparaffinized, rehydrated, and then used to visualize apoptotic bodies. TUNEL staining was performed with the In Situ Apoptosis Detection kit from Millipore-Chemicon International (Temecula, CA) according to the manufacturer's instructions. Four to five random, non-overlapping, non-necrotic fields were imaged and analyzed from each section. The TUNEL-positive apoptotic bodies were quantified by the use of Image ProPlus 5.0 software.

Transmission Electron Microscopy

Dorsolateral prostate tissues from TRAMP mice fed the control diet and the 3 μmol PEITC/g diet were immersion fixed in 2.5% electron microscopy grade glutaraldehyde in PBS overnight at 4°C. Fixed samples were washed three times in PBS, and then post-fixed in 1% aqueous osmium tetroxide containing 0.1% potassium ferricyanide for 1 hour. Following three PBS washes, samples were dehydrated through a graded series of 30%–100% ethanol. Propylene oxide (100%) was then infiltrated in a 1:1 mixture of propylene oxide and Polybed 812 epoxy resin (Epon) (Polysciences, Warrington, PA) for 1 hour. After several changes of 100% resin over 24 hours, samples were embedded in molds, cured at 37°C overnight, followed by additional hardening at 65°C for 2 days. Ultrathin (60 nm) sections were collected on 200 mesh copper grids, stained with 2% uranyl acetate in 50% methanol for 10 minutes, then stained in 1% lead citrate for 7 minutes. Sections were imaged by the use of a JEOL JEM 1011 transmission electron microscope (Peabody, MA) at 80 kV fitted with a side-mount AMT 2k digital camera (Advanced Microscopy Techniques, Danvers, MA).

Plasma Proteomics by the Use of Two-Dimensional Gel Electrophoresis and Mass Spectrometry

Proteomic analyses of plasma samples collected from the TRAMP mice fed the control diet (n = 3) and the 3 μmol PEITC/g diet (n = 3), matched by prostate weights, were conducted by two-dimensional gel electrophoresis followed by mass spectrometry (Applied Biomics, Hayward, CA). Briefly, the samples were thawed, vortexed for 20 seconds, and then subjected to centrifugation at 12 000*g* for 30 minutes at 4°C. The supernatant fraction (1 μL) was mixed with 5 μL of lysis buffer (7 mM urea, 2 mM thiourea, 4% CHAPS, and 30 mM Tris–HCl, at pH 8.5) before labeling with 1 μL of diluted CyDye (1:5 dilution) (GE Healthcare, Piscataway, NJ). Samples were vortexed and incubated on ice in the dark for 30 minutes, after which 1 μL of 10 mM lysine was added. Samples were vortexed, and incubated in the dark on ice for another 15 minutes. The Cy2-, Cy3-, and Cy5-labeled samples were then mixed with sample buffer (8 M urea, 4% CHAPS, 20 mg/mL dithiothreitol, 2% pharmalytes, and trace amount of bromophenol blue) and subjected to rehydration to 250 μL for the 13-cm IPG strip. The protocol provided by GE Healthcare (previously Amersham Biosciences) was followed, and the isoelectric focusing was performed in the dark at 20°C. Images were scanned immediately following sodium dodecyl sulfate–polyacrylamide gel electrophoresis with the use of Typhoon TRIO (GE Healthcare) following the protocols provided by the manufacturer. The scanned images were analyzed by Image Quant software (version 5.0, GE Healthcare) and subjected to in-gel analysis and cross-gel analysis with the use of DeCyder software (version 6.0, GE Healthcare). Results are expressed as a ratio of abundance of a desired protein in the 3 μmol PEITC/g diet group compared with the control diet group.

Selected spots were identified by Ettan Spot Picker (GE Healthcare) following the DeCyder software analysis and spot picking criteria selection. The selected protein spots were subjected to in-gel trypsin digestion, peptide extraction, and desalting followed by MALDI-TOF/TOF (Applied Biosystems, Carlsbad, CA) to identify the isolated protein.

Changes in clusterin levels were verified with the use of plasma samples from seven TRAMP mice that were fed the control diet and eight mice that were fed the 3 μmol PEITC/g diet (three original samples used for proteomics analysis were also analyzed for changes in clusterin levels) with the use of a rat clusterin ELISA kit, according to the manufacturer's protocol (Life Diagnostics, West Chester, PA).

Cell Line and Treatments

TRAMP-C1 cells (a generous gift from Dr Barbara Foster, University of Pittsburgh, Pittsburgh, PA; currently at the Roswell Park Cancer Institute, Buffalo, NY) were cultured in Dulbecco's modified essential medium supplemented with 10% heat-inactivated fetal bovine serum, 1×10^{-8} mM 5α-androstan-17β-ol-3-one, and antibiotics. The TRAMP-C1 cell line was established by Foster et al. (33) from the tumor of a 32-week-old TRAMP mouse. This cell line expresses cytokeratin, E-cadherin, and the androgen receptor and is tumorigenic when implanted in syngeneic C57BL/6 mice (33). Expression of the T antigen is not detectable in TRAMP-C1 cells in vitro or in vivo (33). Cell line authentication was done by Research Animal Diagnostic Laboratory (University of Missouri, Columbia, MO). TRAMP-C1 cells were positive for mouse genomic DNA, but no mammalian interspecies contamination was detected. A genetic profile was generated by the use of a panel of microsatellite markers for genotyping. TRAMP-C1 cells were last tested in August 2010.

Western Blotting for Clusterin Protein Expression

Western blotting for clusterin protein expression in conditioned media and lysates of TRAMP-C1 cells after 24 hours of treatment with dimethyl sulfoxide (DMSO) (control) or PEITC, D,L-sulforaphane, allyl isothiocyanate, benzyl isothiocyanate, diallyl trisulfide, or gluconasturtiin was performed essentially as described previously (34). Briefly, TRAMP-C1 cells (3×10^5 cells per well) were plated in six-well plates and allowed to attach for overnight. The cells were then exposed to DMSO (control) or PEITC (1, 2.5, or 5 μM), D,L-sulforaphane (10 or 20 μM), allyl isothiocyanate (2.5 or 5 μM), benzyl isothiocyanate (2.5 or 5 μM), diallyl trisulfide (20 or 40 μM), or gluconasturtiin (2.5 or 5 μM) for 24 hours. Concentrations of different agents were selected because of published literature accounting for their growth inhibitory and proapoptotic activities (24,31,35). Conditioned media were prepared by centrifugation at 1300*g* for 10 minutes at 4°C. Following treatment, cells were washed twice with ice-cold PBS and lysed on ice with a solution containing 50 mM Tris, 1% Triton X-100, 0.1% sodium dodecyl sulfate, 150 mM NaCl, protease inhibitors, and phosphatase inhibitors. The cell lysate was cleared by centrifugation at 14 000*g* for 15 minutes. Protein concentration was determined with the use of Bradford reagent (Bio-Rad, Hercules, CA). Aliquot containing 50 μg protein was subjected to sodium dodecyl sulfate–polyacrylamide gel electrophoresis. The proteins were transferred onto polyvinylidene fluoride membrane (Perkin Elmer, Boston, MA). After blocking with 5% nonfat dry milk in Tris-buffered saline containing 0.05% Tween-20 (Bio-Rad), the membrane was incubated with clusterin antibody overnight at 4°C. Subsequently, the membrane was incubated with goat secondary antibody, and the immunoreactive protein bands were visualized by the use of the Enhanced

Chemiluminescence kit (NEN Life Science Products, Boston, MA) according to the manufacturer's instructions. Each membrane was stripped and reprobed with anti-actin antibody to correct for differences in protein loading. The western blotting experiment was repeated four to five times with independently prepared lysates from two to three different cell treatment experiments.

Statistical Analysis

All *P* values presented correspond to two-sided hypothesis tests. Statistical analysis for body weight and diet consumption over time was performed by use of a mixed-effects analysis of variance (ANOVA) where PEITC concentrations (0, 1.5, or 3 μmol PEITC/g diet) and duration of treatment (1–19 weeks) were categorical fixed effects, and each mouse was a categorical random effect. The statistical significance for differences in PEITC levels in plasma and prostate was determined by Wilcoxon rank sum test. Statistical significance for differences among the groups in mean vital organ weight, and urogenital and prostate weight was assessed by ANOVA with Dunnett adjustment for multiple comparisons. Statistical significance for differences in the number of TUNEL-positive bodies and number of vessels (CD31-positive vessels), and expression of T antigen, Ki-67, LC3, p62, or E-cadherin were determined by the mixed-effects ANOVA with Dunnett adjustment (Dunnett adjustment was not applied for p62). The effect of PEITC administration on the incidence of different histopathologies identified as normal, PIN, WD, or PD was evaluated by mixed-effects logistic regression, for which diet (control vs PEITC-supplemented) was considered a fixed effect (ie, a variable of analytic interest), and mouse and microscopic fields (within mouse) were considered normally distributed random effects. The effect of PEITC administration on the burden (affected area) of different histopathologies was determined by mixed-effects ANOVA with Dunnett adjustment (36). Percent area (affected area) corresponding to normal gland, PIN, WD, and PD was computed by analysis of 10 randomly selected, non-overlapping, non-necrotic fields on H&E-stained sections of the dorsolateral prostate of each TRAMP mouse. The number of lung metastases and autophagosomes were analyzed by Poisson ANOVA, which is appropriate for count data. Differences were considered statistically significant at *P* less than .05. All analyses were performed using SAS v9.2 software (SAS Institute, Cary, NC).

Results

Safety and Tissue Concentrations

Initially, we used nontransgenic littermates (wild-type male mice) to assess the safety of dietary PEITC administration (3 μmol PEITC/g diet for 19 weeks starting at 5 weeks of age). As shown in Figure 1, A, the PEITC administration did not affect histology of the lateral or dorsal prostate, which are the primary sites of prostate cancer development in the TRAMP model (28,29), and considered most similar to the peripheral zone of the human prostate where most carcinomas occur (37). Diet consumption (results not shown) was comparable for the wild-type mice placed on control and PEITC-supplemented diets. Mice fed the control diet (n = 6) gained more weight over time compared with mice fed the PEITC-supplemented diet (n = 6), but the difference was non-statistically significant (*P* = .11) (Figure 1, B). The histology of the vital organs (liver, lung, kidney, heart, spleen) was normal for the PEITC-fed mice (results not shown). PEITC was detectable in both plasma (mean = 1451 nM, 95% confidence interval [CI] = 696 to 2206 nM) and the prostates (mean = 1138 nmol/kg, 95% CI = 352 to 1925 nmol/kg) of mice fed the 3 μmol PEITC/g diet (n = 3) (Figure 1, C). As expected, the PEITC concentration was below the lower limit of quantitation in the plasma and prostates of mice fed the control diet (n = 3) (Figure 1, C).

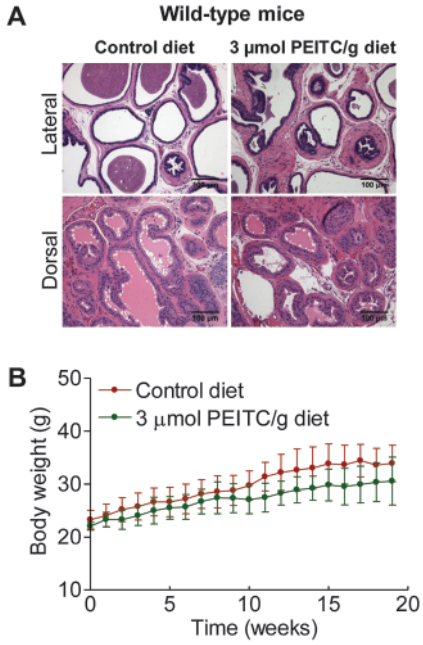

C

Sample	PEITC content	
	mean	95% CI
Prostate – control	0* [nmol/kg]	-
Prostate – PEITC	1138 [nmol/kg]	352 to 1925
Plasma – control	0* [nM]	-
Plasma – PEITC	1451 [nM]	696 to 2206

Figure 1. Safety and tissue levels of phenethyl isothiocyanate (PEITC) in wild-type (nontransgenic) male mice. **A**) Representative sections stained with hematoxylin and eosin of dorsal and lateral prostate from wild-type (nontransgenic) male mice fed either control diet or diet supplemented with 3 μmol PEITC/g for 19 weeks. Scale bar = 100 μm. **B**) Body weights over time of wild-type (nontransgenic) male mice fed control diet or diet supplemented with 3 μmol PEITC/g (n = 6 mice per group). Mean body weights with 95% confidence intervals (**error bars**) are shown. Statistical significance between control diet group and PEITC-supplemented diet groups was determined by two-sided mixed-effects analysis of variance (*P* = .11). **C**) Levels of PEITC in the plasma and prostate of wild-type (nontransgenic) male mice (n = 3 mice per group). *P* = .10 for both the plasma and the prostate between control and PEITC groups by Wilcoxon rank sum test. PEITC content below the lower limit of quantitation (**asterisk**). All statistical tests were two-sided.

Effect of Dietary PEITC on Prostate Cancer Development in TRAMP Mice

We next designed experiments to investigate a concentration–effect relationship for dietary PEITC administration on tumor

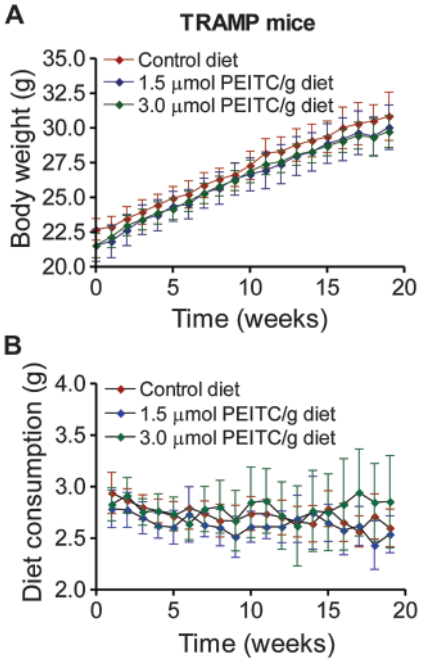

Figure 2. Effect of dietary phenethyl isothiocyanate (PEITC) administration on body weight in mice transgenic for prostate adenocarcinoma. **A**) Body weights over time of male transgenic mice fed either control diet or diet supplemented with the indicated concentrations of PEITC. Mean body weights and their 95% confidence intervals (**error bars**) are shown (n = 21 for mice fed control diet and 3 µmol PEITC/g diet, n = 19 for mice fed 1.5 µmol PEITC/g diet). **B**) Diet consumption over time by mice fed control diet and PEITC-supplemented diets. Mean diet consumptions and their 95% confidence intervals (**error bars**) are shown (n = 21 for mice fed control diet and 3 µmol PEITC/g diet, n = 19 for mice fed 1.5 µmol PEITC/g diet).

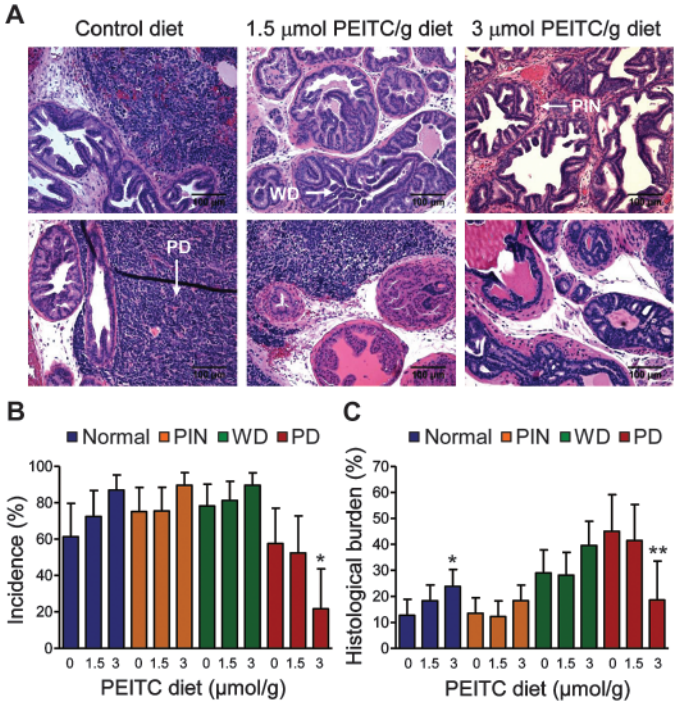

Figure 3. Effect of dietary phenethyl isothiocyanate (PEITC) administration on incidence and burden (affected area) of prostatic intraepithelial neoplasia (PIN), well differentiated carcinoma (WD), and poorly differentiated cancer (PD) in the dorsolateral prostate of mice transgenic for adenocarcinoma. **A**) Representative sections stained with hematoxylin and eosin of the dorsolateral prostate from control and PEITC-treated mice (×200 magnification). Areas consistent with PIN, WD, and PD are shown (**arrows**). Scale bar = 100 µm. **B**) Incidence (percent mice with histological evidence) of normal prostate (normal), low- and high-grade PIN, WD, and PD in the dorsolateral prostate of mice fed the control diet or the PEITC-supplemented diet (n = 19 for control diet [0 µmol PEITC/g diet] and 1.5 µmol PEITC/g diet groups, and n =18 for the 3 µmol PEITC/g diet group). *Statistically significantly different ($P = .04$) compared with control diet group by mixed-effects analysis of variance (ANOVA) with Dunnett adjustment. **C**) Percent area (affected area) of prostate gland occupied by the normal prostate (normal), PIN, WD, or PD carcinoma (n =19 for the control diet and 1.5 µmol PEITC/g diet groups, and n = 18 for the 3 µmol PEITC/g diet group). Ten random, non-overlapping, and non-necrotic fields from each section were scored by two independent investigators. *Statistically significantly different ($P = .03$) compared with control by mixed-effects ANOVA with Dunnett adjustment. **Statistically significantly different ($P = .02$) compared with control by mixed-effects ANOVA with Dunnett adjustment. All statistical tests were two-sided.

development in TRAMP mice. Five-week-old male TRAMP mice were placed on the control diet or a diet supplemented with 1.5 or 3 µmol PEITC/g for 19 weeks. There was a systematic change in body weight over time in all three groups (Figure 2, A), but the difference was non-statistically significant ($P \geq .4$ by two-sided mixed effects ANOVA). Moreover, the PEITC-supplemented diet was well tolerated by the TRAMP mice and did not result in any toxic effects as evidenced by no change in the weight of vital organs (Supplementary Table 1, available online). However, a trend of a dose-dependent decrease in mean weights of the urogenital tract and prostate in the mice fed PEITC-supplemented diet compared with control was observed, although the difference did not reach statistical significance (Supplementary Table 1, available online). Diet consumption was comparable in all three groups (Figure 2, B).

Representative H&E-stained sections from the dorsolateral prostate of TRAMP mice fed control and PEITC-supplemented diets are shown in Figure 3, A. The dorsolateral prostate of TRAMP mice revealed the presence of PIN, WD, and PD areas identified by arrows in Figure 3, A. The incidence of PD was decreased in the mice fed 3 µmol PEITC/g diet group by 62.40% as compared with the mice fed control diet (3 µmol PEITC/g diet vs control diet, mean = 21.65% vs 57.58%, difference = −35.93%, 95% CI = −45.48% to −13.10%, $P = .04$ by two-sided mixed-effects ANOVA with Dunnett adjustment) (Figure 3, B). The histological burden (affected area) associated with PD was statistically significantly lower in the 3 µmol PEITC/g diet group mice compared with the control mice (3 µmol PEITC/g diet vs control diet, mean = 18.53% vs 45.01%, difference = −26.48%, 95% CI = −49.78% to −3.19%, $P = .02$ by two-sided mixed-effects ANOVA with Dunnett adjustment) (Figure 3, C). In addition, we observed a trend of an increase in the area occupied by the histological features consistent with WD, PIN, and normal tissue when comparing mice in the control group with those in the 3 µmol PEITC/g diet group (Figure 3, C). Moreover, the histological burden of normal prostate was statistically significantly higher in the mice fed 3 µmol PEITC/g diet compared with control mice (3 µmol PEITC/g diet vs control diet, mean = 23.75% vs 12.61%, difference = 11.14%, 95% CI = 0.92% to 21.37%,

P = .03 by two-sided mixed-effects ANOVA with Dunnett adjustment) (Figure 3, C). Together, these results indicate that a PEITC-supplemented diet at the 3 μmol dose inhibits the progression to PD, which is a clinically significant finding, because the majority of prostate cancer mortality is associated with advanced disease.

Effect of PEITC Administration on Cell Proliferation

Prostate cancer in TRAMP mice is driven by the prostate epithelial-specific expression of T/t antigen driven by the minimal rat probasin promoter (28). Initially, we considered a possibility that the PEITC-mediated inhibition of prostate cancer progression was because of suppression of T-antigen expression. As shown in Figure 4, A, expression of the T antigen was non-statistically significantly decreased by the dietary PEITC administration (3 μmol PEITC/g diet vs control diet, mean = 1156 vs 1268 T antigen–positive cells per field, difference = −112 T antigen–positive cells per field, 95% CI = −576.90 to 352.88 T antigen–positive cells per field, P = .81 by two-sided mixed-effects ANOVA with Dunnett adjustment). Because in vitro cellular studies have documented the antiproliferative, proapoptotic, and anti-angiogenic activity of PEITC (20,21,23,27), we performed immunohistochemical staining for Ki-67 (a well-known proliferation marker), TUNEL-positive bodies (a marker of apoptosis), and CD31 (a marker of neoangiogenesis). Cell proliferation, as assayed by Ki-67 expression, in TRAMP mice that were fed a diet supplemented with 3 μmol PEITC/g diet was reduced by 41.11% compared with that in mice that were fed the control diet, but the difference was not statistically significant (3 μmol PEITC/g diet vs control diet, mean = 536.8 vs 911.6 Ki-67-positive cells per field, difference = −374.8 Ki-67-positive cells per field, 95% CI = −811.92 to 62.30 Ki-67-positive cells per field, P = .10 by two-sided mixed-effects ANOVA with Dunnett adjustment (Figure 4, B). In contrast to cellular data (20,21,23), the mean number of TUNEL-positive bodies were comparable in the dorsolateral prostate of TRAMP mice fed 3 μmol PEITC/g diet and control diet (3 μmol PEITC/g diet vs control diet, mean = 111.4 vs 113.3 TUNEL-positive bodies per field, difference = −1.9 TUNEL-positive bodies per field, 95% CI = −40.62 to 36.91 TUNEL-positive bodies per field, P = .99 by two-sided mixed-effects ANOVA with Dunnett adjustment) (Figure 4, C). In addition, the average number of blood vessels observed in the dorsolateral prostate sections of TRAMP mice did not differ between mice that were fed the control diet and those that were fed the 3 μmol PEITC/g diet (3 μmol PEITC/g diet vs control diet, mean = 34.0 vs 40.79 vessels per field, difference = −6.79 vessels per field, 95% CI = −18.85 to 5.27 vessels per field, P = .34 by two-sided mixed-effects ANOVA with Dunnett adjustment) (Figure 4, D). However, morphology of the vessels was markedly altered in the sections of TRAMP mice fed the 3 μmol PEITC/g diet compared with mice fed the control diet. Specifically, the vessels appeared to be more rounded and "regular" in shape in the dorsolateral prostate of TRAMP mice fed the 3 μmol PEITC/g diet as opposed to the irregular vessels predominant in the dorsolateral prostate of TRAMP mice fed the control diet (Figure 4, D). It is important to point out that meandering and irregularly shaped blood vessels are a feature of the tumor vasculature shown to be predictive of prostate cancer progression (38).

Effect of PEITC Administration on Induction of Autophagy

We have previously shown that PEITC treatment causes autophagic cell death in cultured PC-3 and LNCaP human prostate cancer cells and is characterized by the accumulation of autophagosomes and increased expression of the autophagy regulator LC3 (25). As shown in Figure 5, A, we observed a statistically significant increase in the average number of autophagosomes in the dorsolateral prostate of TRAMP mice fed the 3 μmol PEITC/g diet (n = 40) compared with the mice fed the control diet (n = 32) (3 μmol PEITC/g diet vs control diet, mean = 5.75 vs 2.84 autophagosomes per high-power field, difference = 2.91 autophagosomes per high-power field, 95% CI = 2.06 to 3.71 autophagosomes per high-power field, P < .001 by two-sided Poisson ANOVA). We next determined the effect of PEITC administration on the expression of p62 (also known as p62/SQSTM1 or sequestosome 1) because defective autophagy leads to accumulation of this protein (39). Expression of p62 was lower in the dorsolateral prostate of TRAMP mice fed the 3 μmol PEITC/g diet (n = 5) as compared with the control diet (n = 5) (3 μmol PEITC/g diet vs control diet, mean = 2.12% vs 6.33% p62-positive area, difference = −4.21% p62-positive area, 95% CI = −11.87% to 3.45% p62-positive area), although the difference was non-statistically significant (P = .24 by two-sided mixed-effects ANOVA) because of large variability (Figure 5, B). Dorsolateral prostate from TRAMP mice fed the 3 μmol PEITC/g diet (n = 18) exhibited a statistically significant increase in expression of LC3 protein compared with control group (n = 19) (3 μmol PEITC/g diet vs control diet, mean = 23.36% vs 5.36% LC3-positive area, difference = 18.0% LC3-positive area, 95% CI = 10.39% to 25.61% LC3-positive area, P < .001 by mixed-effects ANOVA with Dunnett adjustment) (Figure 5, C). Western blotting of tissue lysates from the dorsolateral prostate of TRAMP mice also revealed an increase in the expression of total as well as cleaved 16-kDa LC3 (results not shown). Together, these results provided in vivo evidence for PEITC-induced autophagy in the dorsolateral prostate of TRAMP mice.

Effect of PEITC Administration on E-cadherin Expression

E-cadherin is considered a suppressor of invasion and growth in many epithelial cancers (40). Expression of E-cadherin was statistically significantly higher in the dorsolateral prostate of TRAMP mice fed 3 μmol PEITC/g diet (n = 18) compared with mice fed control diet (n = 18) (3 μmol PEITC/g diet vs control diet, mean = 31.45% vs 18.21% E-cadherin-positive area, difference = 13.24% E-cadherin-positive area, 95% CI = 3.02% to 23.46% E-cadherin-positive area, P = .009 by two-sided mixed-effects ANOVA with Dunnett adjustment) (Figure 6, A).

Effect of PEITC Administration on Lung Metastasis

Because PEITC administration resulted in induction of E-cadherin expression (Figure 6, A), we proceeded to score incidence of pulmonary metastasis and number of lung metastasis per mouse (multiplicity) in mice fed either the control diet or 3 μmol PEITC/g diet. Figure 6, B shows representative H&E-stained lung sections from mice fed control or 3 μmol PEITC/g diet. Overall incidence of pulmonary metastasis did not differ between the control and PEITC groups (data not shown). The number of lung metastasis

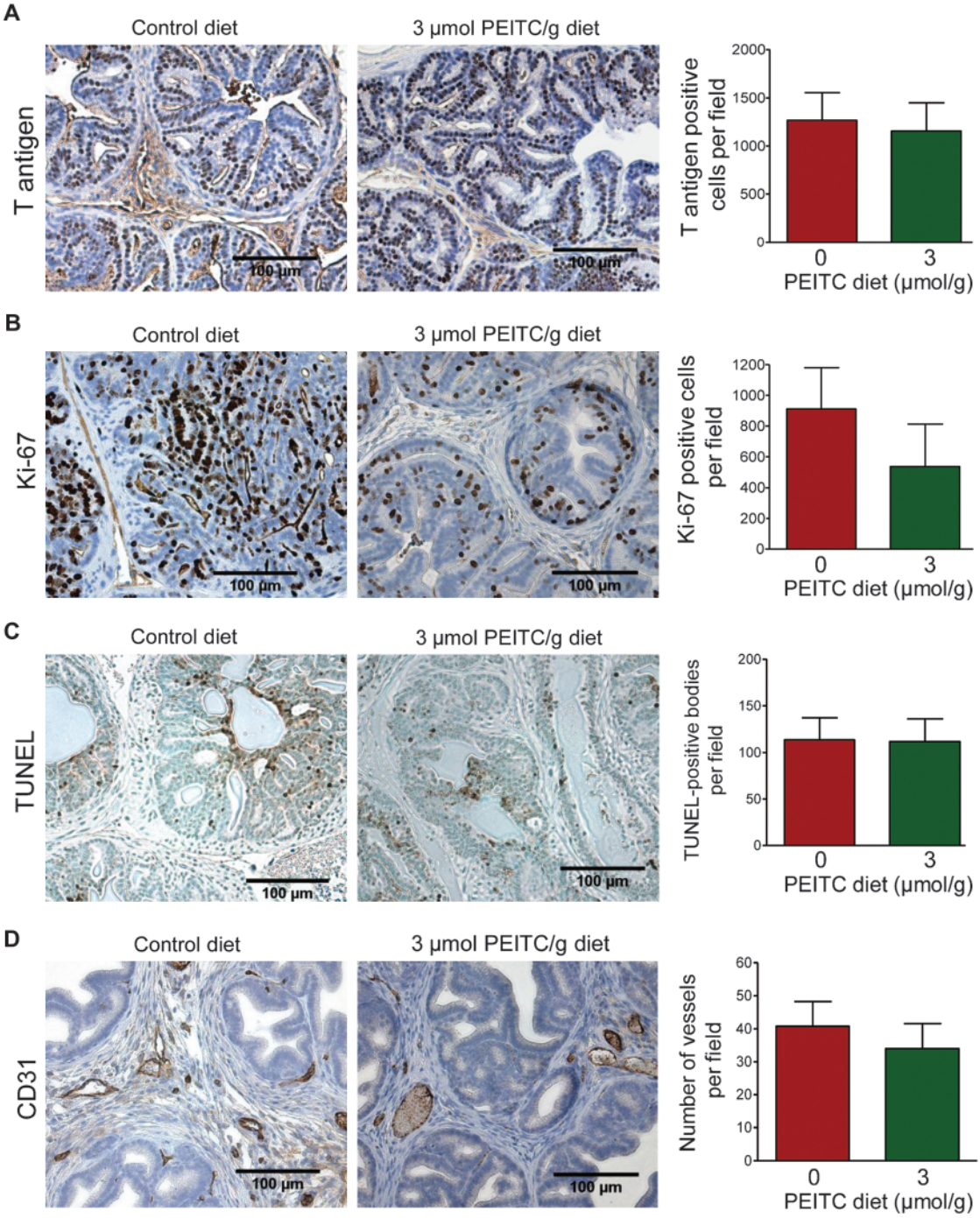

Figure 4. Effect of phenethyl isothiocyanate (PEITC) administration on cell proliferation, apoptosis, and neovascularization in the dorsolateral prostate of mice transgenic for prostate adenocarcinoma. Immunohistochemical analysis for **A**) T antigen expression (n = 19 for control and n = 18 for PEITC; $P = .81$), **B**) Ki-67 expression (marker of cellular proliferation, n = 19 for control and n = 18 for PEITC; $P = .10$), **C**) terminal deoxynucleotidyl transferase–mediated dUTP nick-end labeling (TUNEL)–positive bodies (n = 19 for control and n = 18 for PEITC; $P = .99$), and **D**) number of vessels (CD31 positive) (n = 19 for control and n = 18 for PEITC; $P = .34$) in the dorsolateral prostate of mice fed control diet or 3 μmol PEITC/g diet (×200 magnification, scale bar = 100 μm). Mean positive cells per field (T antigen and Ki-67), mean TUNEL-positive bodies per field, mean number of vessels per field, and corresponding 95% confidence intervals (**error bars**) are shown. *P* values were calculated by using two-sided mixed-effects analysis of variance with Dunnett adjustment.

per mouse in the mice fed the 3 μmol PEITC/g diet (n = 21) was 38.37% lower than that in mice fed the control diet (n = 20) (3 μmol PEITC/g diet vs control diet, mean = 1.14 vs 1.85 lung metastasis per mouse, difference = −0.71 lung metastasis per mouse, 95% CI = −2.0 to 0.42 lung metastasis per mouse, $P = .07$ by two-sided Poisson ANOVA) (Figure 6, B). In addition, the area occupied by the pulmonary metastasis was generally smaller in the prostates of the TRAMP mice fed the 3 μmol PEITC/g diet compared with those of mice fed the control diet, reflected by an approximate 60% reduction in the mean pulmonary metastasis area

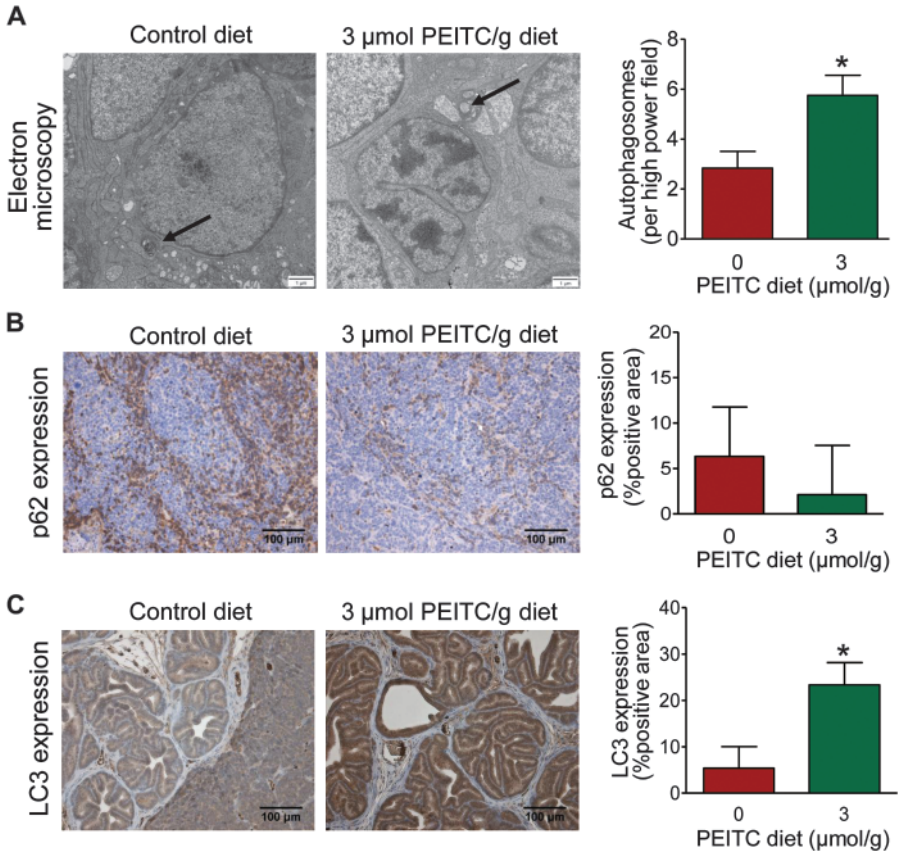

Figure 5. Effect of phenethyl isothiocyanate (PEITC) administration on markers of autophagy in the dorsolateral prostate of mice transgenic for prostate adenocarcinoma. **A**) Representative electron micrographs of dorsolateral prostate tissues from mice fed the control diet or the 3 µmol PEITC/g diet and corresponding bar graphs of markers are shown. Autophagosomes are identified by **arrows** (×15 000 magnification). The **bar graph** represents mean number of autophagosomes per field with 95% confidence intervals (**error bars**) (n = 32 fields from tissues of two mice fed the control diet and n = 40 fields from tissues of three mice fed the 3 µmol PEITC/g diet). Scale bar = 1 µm. **P* < .001 (Poisson analysis of variance [ANOVA]). **B**) p62 expression (×200 magnification). The **bar graph** represents mean percent positive area with 95% confidence intervals (n = 5 for both groups). Scale bar = 100 µm. *P* = .24 (mixed-effects ANOVA). **C**) LC3 expression (×200 magnification). The **bar graph** represents mean percent positive area and 95% confidence intervals (**error bars**; n = 19 for mice fed the control diet, and n = 18 for mice fed the 3 µmol PEITC/g diet). Scale bar = 100 µm. **P* < .001 (mixed-effects ANOVA with Dunnett adjustment). All statistical tests were two-sided.

(data not shown). Despite the lack of statistical significance for difference in number of lung metastasis per mouse, E-cadherin may be a viable marker for the assessment of biological response in the prostate to PEITC administration in future clinical trials.

Plasma Proteomics

Using a plasma proteomics approach, we set out to identify measurable biomarkers of PEITC response potentially useful in future clinical trials. Plasma samples from TRAMP mice fed the control or 3 µmol PEITC/g diet (n = 3), matched by prostate weight, were analyzed by two-dimensional gel electrophoresis to identify differentially expressed proteins. Several non-abundant proteins were identified to be differentially expressed in the plasma of control and PEITC-fed mice (Table 1). One of the proteins affected by PEITC treatment was identified to be clusterin. These initial results were confirmed by ELISA, which revealed a statistically significant decrease in clusterin in the plasma of TRAMP mice fed 3 µmol PEITC/g diet (n = 8) compared with mice fed control diet

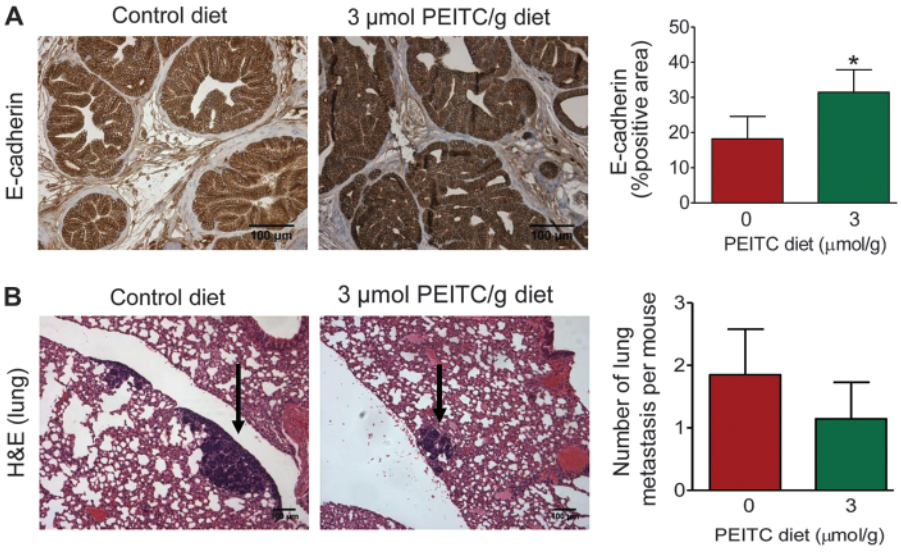

Figure 6. Effect of phenethyl isothiocyanate (PEITC) administration on E-cadherin expression in the dorsolateral prostate and lung metastasis in mice transgenic for prostate adenocarcinoma. **A**) E-cadherin expression (×200 magnification). The **bar graph** represents mean percent positive area with 95% confidence intervals (n = 18 for both groups). Scale bar = 100 µm. **P* = .009 (mixed-effects analysis of variance [ANOVA] with Dunnett adjustment). **B**) Representative sections stained with hematoxylin and eosin (H&E) depicting lung metastasis (**arrows**) in a representative mouse fed control diet or 3 µmol PEITC/g diet (×100 magnification). **Bar graph** depicts mean number of lung metastasis per mouse with 95% confidence intervals (**error bars**) (n = 20 for mice fed the control diet and n = 21 for mice fed the 3 µmol PEITC/g diet). Scale bar = 100 µm. *P* = .07 (Poisson ANOVA). All statistical tests were two-sided.

Table 1. Non-abundant plasma proteins altered by phenethyl isothiocyanate (PEITC) administration in mice transgenic for prostate adenocarcinoma

Protein name	Master No.	Protein ID	Ratio of protein abundance, PEITC vs control*	*P*†
Chain A, crystal structure of mouse transthyretin	2058	23	−1.98	.004
Alpha-fetoprotein	771	10	1.34	.01
Alpha-fetoprotein	367	4	1.25	.01
Chain A, crystal structure of mouse transthyretin	1795	20	−1.73	.03
Transferrin (*Mus musculus*)	1191	18	1.28	.03
Alpha-fetoprotein	673	11	1.29	.03
Clustrin	1033	12	1.55	.04
Actin filament associated protein 1-like 2 (*M musculus*)	181	2	1.34	.049
Alpha-fetoprotein	371	3	1.29	.05
Alpha-fetoprotein	725	9	1.34	.06
Plasminogen, isoform CRA_e (*M musculus*)	78	1	−1.31	.06
Clusterin (*M musculus*)	681	8	−1.33	.07
Alpha-fetoprotein	415	6	1.31	.07
Transferrin (*M musculus*)	533	7	1.57	.09
Apolipoprotein A-I, isoform CRA_b (*M musculus*)	2350	25	1.32	.08

* Plasma specimens were from mice fed either control diet or 3 μmol PEITC/g diet (n = 3 mice per group).

† All *P* values were calculated by a two-sided Student *t* test.

(n = 7) (3 μmol PEITC/g diet vs control diet, mean = 223.0 vs 851.9 ng/mg protein, difference = −628.9 ng/mg protein, 95% CI = −1161.81 to −95.82 ng/mg protein, $P = .02$ by two-sided mixed-effects ANOVA (Figure 7, A). Next, to determine the effect of PEITC treatment on both the intracellular and secreted forms of clusterin, a TRAMP tumor-derived cell line (TRAMP-C1) was

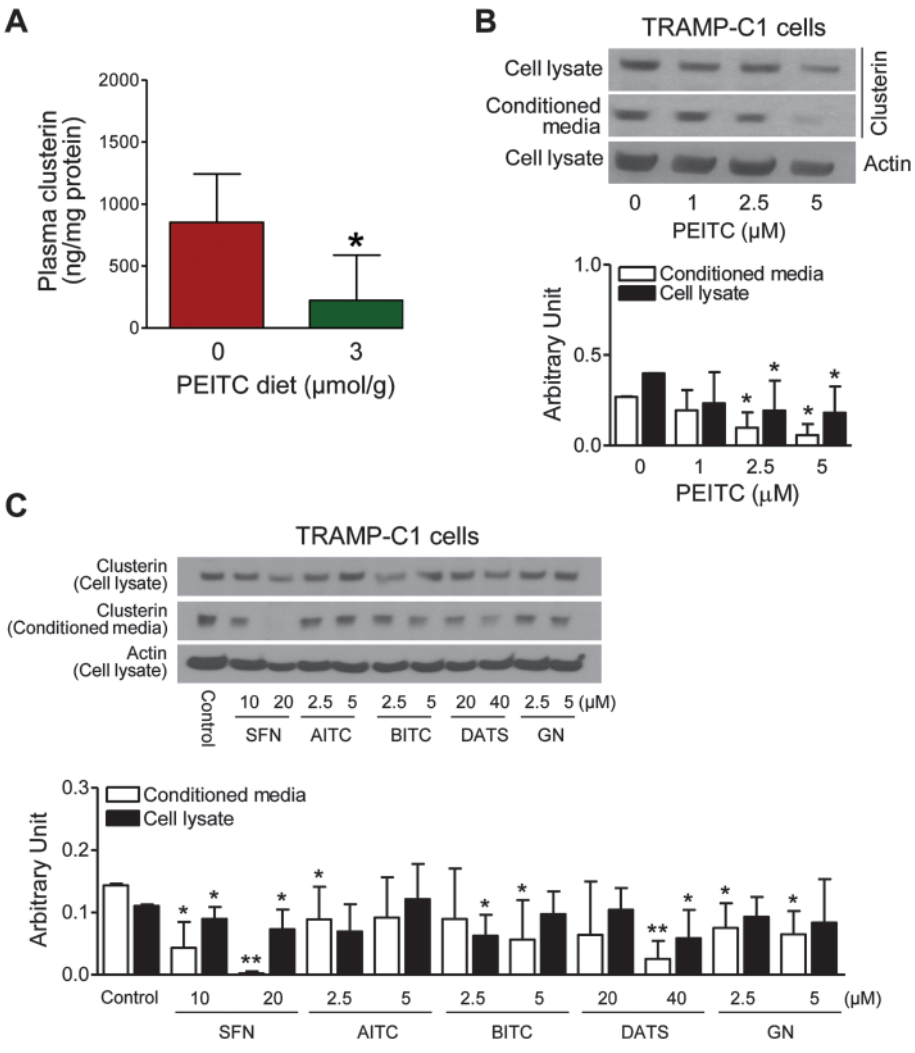

Figure 7. Effect of phenethyl isothiocyanate (PEITC) administration on clusterin protein expression in plasma of mice transgenic for prostate adenocarcinoma. **A**) Clusterin levels in the plasma of mice fed control or 3 μmol PEITC/g diet. Results shown are mean plasma clusterin (ng/mg protein) with 95% confidence intervals (**error bars**) (n = 7 for mice fed the control diet and n = 8 for mice fed the 3 μmol PEITC/g diet). **P* = .02 (two-sided mixed-effects analysis of variance). **B**) Detection of clusterin protein by western blotting of cell lysates and conditioned media from TRAMP-C1 cells treated for 24 hours with the indicated concentrations of PEITC. Actin was used as a loading control. **Bar graph** shows mean (arbitrary units) and 95% confidence intervals (**error bars**). (n = 4 from lysates prepared from three different batches). **P* ≤ .05 (two-sided Student *t* test). **C**) Detection of clusterin protein levels by western blotting of cell lysates and conditioned media from TRAMP-C1 cells treated for 24 hours with 10 and 20 μM D,L-sulforaphane (SFN), 2.5 and 5 μM allyl isothiocyanate (AITC), 2.5 and 5 μM benzyl isothiocyanate (BITC), 20 and 40 μM diallyl trisulfide (DATS), and 2.5 and 5 μM gluconasturtiin (GN). Actin was used as a loading control. **Bar graph** shows mean (arbitrary units) and 95% confidence intervals (**error bars**) (n = 5 from lysates prepared from two different batches). **P* ≤ .05 and ***P* ≤ .001 (two-sided Student *t* test).

studied. As shown in Figure 7, B, PEITC treatment resulted in a concentration-dependent decrease in clusterin protein levels in the lysates and conditioned media of TRAMP-C1 cells in vitro. Compared with control (0 μM PEITC, 24 hours) (n = 4), TRAMP-C1 cells treated for 24 hours with 2.5 μM PEITC (n = 4) exhibited a statistically significant decrease in the levels of clusterin protein in the conditioned media (2.5 μM PEITC vs control, mean = 0.10 arbitrary unit [AU], 95% CI = 0.01 to 0.18 AU vs mean = 0.27 AU, 95% CI = 0.26 to 0.27 AU, $P = .008$ by two-sided Student *t* test) as well as cell lysate (2.5 μM PEITC vs control, mean = 0.19 AU, 95% CI = 0.03 to 0.36 AU vs mean = 0.40 AU, 95% CI = 0.40 to 0.40 AU, $P = .03$ by two-sided Student *t* test). Twenty-four-hour treatment of TRAMP-C1 cells with 5 μM PEITC (n = 4) also resulted in a statistically significant decrease in the levels of clusterin protein in the conditioned media (5 μM PEITC vs control, mean = 0.06 AU, 95% CI = −0.003 to 0.12 AU vs mean = 0.27 AU, 95% CI = 0.26 to 0.27 AU, $P = .002$ by two-sided Student *t* test) and cell lysate (5 μM PEITC vs control, mean = 0.18 AU, 95% CI = 0.04 to 0.32 AU vs mean = 0.40 AU, 95% CI = 0.40 to 0.40 AU, $P = .02$ by two-sided Student *t* test) compared with control (n = 4) (Figure 7, B).

Next, we determined if clusterin suppression was specific for PEITC treatment or if clusterin suppression was a result of treatment with isothiocyanates in general. A series of compounds that include a thioalkyl-isothiocyanate (D,L-sulforaphane), an aromatic isothiocyanate with close structural similarity to PEITC (benzyl isothiocyanate), a non-aromatic isothiocyanate (allyl isothiocyanate), a non-isothiocyanate compound (diallyl trisulfide), and glucosinolate precursor of PEITC (gluconasturtiin) were tested for their ability to suppress clusterin in TRAMP-C1 cells. Western blotting of conditioned media and cell lysates from TRAMP-C1 cells treated for 24 hours with these compounds revealed differential effects on intracellular vs secreted levels of clusterin by different compounds. For example, as opposed to 5 μM PEITC which statistically significantly reduced clusterin levels in both cell lysate and conditioned media (Figure 7, B), 5 μM allyl isothiocyanate treatment (n = 5) did non-statistically significantly reduce intracellular clusterin (5 μM allyl isothiocyanate vs control, mean = 0.12 AU, 95% CI = 0.06 to 0.18 AU vs mean = 0.11 AU, 95% CI = 0.11 to 0.11 AU, $P = .62$ by two-sided Student *t* test) or clusterin in the conditioned media (5 μM allyl isothiocyanate vs control, mean = 0.09 AU, 95% CI = 0.03 to 0.16 AU vs mean = 0.14 AU, 95% CI = 0.14 to 0.15 AU, $P = .09$ by two-sided Student *t* test) compared with control (n = 5) (Figure 7, C, bar graph). Similarly, treatment (24 hours) with the PEITC precursor gluconasturtiin (n = 5) resulted in a statistically significant suppression of clusterin only in the conditioned media at 2.5 μM dose (2.5 μM gluconasturtiin vs control, mean = 0.08 AU, 95% CI = 0.04 to 0.11 AU vs mean = 0.14 AU, 95% CI = 0.14 to 0.15 AU, $P = .01$ by two-sided Student *t* test) as well as 5 μM dose (5 μM gluconasturtiin vs control, mean = 0.06 AU, 95% CI = 0.03 to 0.10 AU vs mean = 0.14 AU, 95% CI = 0.14 to 0.15 AU, $P = .005$ by two-sided Student *t* test) compared with the control (n = 5) (Figure 7, C). Suppression of clusterin secretion was not unique to isothiocyanate-type compounds because statistically significant suppression of intracellular and secreted clusterin was observed following treatment with 40 μM diallyl trisulfide, which also is an effective inhibitor of prostate cancer development in the TRAMP model (30). Nonetheless, these data indicate that clusterin may be a viable biomarker of PEITC response in future clinical trials.

Discussion

This study demonstrates that dietary PEITC administration is well tolerated in mice, and results in appreciable levels of bioreactive PEITC in the plasma and prostate gland. We also found that male TRAMP mice that were fed a diet supplemented with 3 μmol PEITC/g have a statistically significant decrease in incidence as well as burden (affected area) of PD, which is not because of suppression of T antigen expression.

We found that administration of 3 μmol PEITC/g diet statistically significantly inhibits the incidence as well as burden of PD in the TRAMP model. The 3 μmol dose equates to intake of 8.34 μmol PEITC/mouse/d based on average diet intake of 2.78 g/mouse/d for the mice of this group (Figure 2, B). The PEITC concentrations used in this study are within the range that can be generated by dietary intake of cruciferous vegetables. As reviewed by Hecht (11), glucosinolate content in edible cruciferous vegetables ranges from 0.5 to 3 mg/g and one serving of one ounce watercress is estimated to result in intake of about 37 μmol of PEITC (11).

Suppression of prostate cancer development in TRAMP mice has been demonstrated by us previously with D,L-sulforaphane (31), which is a thioalkyl isothiocyanate compound. Oral gavage with 6 μmol D,L-sulforaphane (3 times per week) inhibits prostate cancer development in TRAMP mice at the PIN and WD stages in association with increased natural killer cell lytic activity (31). The lytic activity of natural killer cells is not increased in PEITC-fed TRAMP mice (A. A. Powolny and S. V. Singh, unpublished observations). These observations underscore critical mechanistic differences in seemingly closely-related compounds. Furthermore, a combination chemoprevention regimen involving D,L-sulforaphane and PEITC may lead to greater chemopreventative activity against prostate cancer development than that observed with the single agents because of their ability to target different stages of the disease as observed in the TRAMP model. Experimental validation of this hypothesis is one of our priorities in future investigations.

The TRAMP model shares many features of human prostate cancer progression, including metastasis to distant sites, progression to androgen independence, and neuroendocrine differentiation (41). The number of neuroendocrine cells in castration-resistant human prostate cancer biopsies is associated with stage, Gleason Grade, and overall survival (42). We found that the fraction of synaptophysin-expressing neuroendocrine cells was not affected by PEITC administration (A. A. Powolny and S. V. Singh, unpublished observations).

Another objective of this study was to determine whether the mechanisms responsible for the anticancer effect of PEITC treatment in cultured human prostate cancer cells are also functional in vivo. Apoptosis induction is readily observed in cultured cancer cells, including TRAMP tumor-derived prostate cancer cell lines, after exposure to PEITC (20,21,23). However, the PEITC administration fails to elicit a proapoptotic response in vivo in the prostatic

tissues of TRAMP mice. Several possibilities exist to explain discrepancies in the results between PEITC studies in cultured human and mouse prostate cancer cell lines and the TRAMP mouse. One such possibility relates to the dose of PEITC administration; a more intensive dosing regimen may be required to elicit a proapoptotic response in vivo. It is also conceivable that, in contrast to cultured cells, the PEITC administration simultaneously provokes certain antiapoptotic mechanisms in vivo (eg, induction of prosurvival pathways, increased expression of inhibitor of apoptosis proteins, etc.) to counteract apoptosis. Additional studies are needed to systematically explore these hypotheses.

This study reveals that PEITC administration regularizes vessel morphology in the tumor without having any statistically significant effect on neoangiogenesis. Mechanisms regulating vasculature morphology are not well understood, but we have previously shown that PEITC treatment reduces the secretion of vascular endothelial growth factor (VEGF) and reduces protein levels of VEGF receptor 2 (VEGF-R2) in human umbilical vein endothelial cells (27). The VEGF/VEGF-R2 signaling axis is one of the key regulators of neoangiogenesis in tumors by the induction of endothelial cell proliferation, increased blood vessel leakiness, and inhibition of pericyte activation and blood vessel maturation (43). A study of neoangiogenesis and the role of the VEGF/VEGF-R2 pathway in a human skin cancer cell line (A-5RT3) transplanted onto the dorsal muscle fascia of nude mice indicated that inhibition of VEGF-R2 by a selective antibody results in suppression of neoangiogenesis and regression of the pre-existing vessels, in association with reduced proliferation of the endothelial cells (44). Moreover, mice treated with the selective anti-VEGF-R2 antibody exhibited normal blood vessel morphology with endothelial cells displaying normal intracellular junctions, complete coverage of pericytes, and a continuous basement membrane (44). These observations imply that inhibition of VEGF-R2 signaling can alter the morphology of the blood vessels in a tumor to resemble that of a normal blood vessel. Therefore, restoration of tumor vessel morphology in response to PEITC treatment may be partially mediated by suppression of the VEGF/VEGF-R2 signaling axis. Additional studies investigating the relationship between PEITC and the VEGF/VEGF-R2 pathway in vivo should be done.

The anticancer effect of PEITC against cultured human prostate cancer cells is associated with Atg5-dependent autophagy in vitro (25). PEITC-mediated cell death in human prostate cancer cell lines is statistically significantly decreased after pharmacological or genetic suppression of autophagy (25), indicating that, unlike certain other anticancer agents including D,L-sulforaphane (45,46), autophagy is not a protective mechanism against apoptosis in prostate cancer cells after treatment with PEITC. This study shows that PEITC mediates autophagy in the TRAMP mouse characterized by the enrichment of autophagosomes and increased expression and processing (cleavage) of LC3. We investigated the effects of PEITC treatment on the p62 protein because of the following: studies have shown that p62 interacts directly with LC3 (47,48); p62 accumulates in mouse models of defective autophagy (49); p62 contributes to the sustained activation of NF-E2-related factor 2 (Nrf2) by creating a positive feedback loop through direct interaction with Keap1 (50–52); and p62 overexpression correlates with an aggressive phenotype in tumors of the breast and prostate (53–55). To determine the effect of the PEITC treatment on p62 status, immunohistochemical analysis for p62 protein expression revealed a non-statistically significant decrease ($P = .24$) in the expression of p62 in the prostate tumors of TRAMP mice fed a PEITC-supplemented diet compared with mice fed the control diet. These markers of autophagy may also serve as endpoints to assess biological activity of PEITC in future clinical investigations.

E-cadherin plays an important role in normal physiological processes including development, cell polarity, and tissue morphology (56). E-cadherin is considered a tumor suppressor because of its role in inhibition of epithelial to mesenchymal transition (57). E-cadherin is frequently downregulated during cancer progression and is associated with poor prognosis (58). This study reveals that dietary PEITC administration causes a statistically significant increase ($P = .009$) in expression of E-cadherin in the dorsolateral prostate of TRAMP mice. Thus, it is reasonable to conclude that E-cadherin overexpression contributes to the chemopreventative activity induced by dietary PEITC administration in the TRAMP mouse. A non-statistically significant ($P = .07$) yet marked decrease in number of lung metastasis per mouse provides further evidence to support this hypothesis. Future studies are needed to elucidate the mechanism of PEITC-mediated induction of E-cadherin protein expression and to test if PEITC treatment inhibits epithelial to mesenchymal transition in preclinical models of prostate cancer.

Our data also showed that the levels of several plasma proteins, including clusterin, were changed after PEITC administration in TRAMP mice. Clusterin (also known as apolipoprotein J and testosterone-repressed prostate message-2) is a highly conserved protein expressed in a variety of tissues, secreted in blood, and involved in regulation of apoptosis, cell adhesion, cell cycle regulation, and DNA repair (59,60). Increased levels of clusterin have been reported in several malignancies, including breast, colon, lung, and prostate cancers (59). Furthermore, increased clusterin levels were previously shown to be associated with a higher Gleason score in prostate cancer patients (60). However, a recent study argues that clusterin may act as a prostate tumor suppressor based on results in clusterin knockout mice and clusterin knockout mice crossed with TRAMP (C57BL/6J background) mice (61). Clusterin knockout mice exhibit transformation of the prostate epithelium and crossing of clusterin knockout mice with TRAMP mice results in increased metastatic spread (61). However, these studies did not differentiate between the two forms of clusterin—secreted, glycosylated clusterin, and nonglycosylated clusterin that is localized to the nucleus and mitochondria (59). Secreted clusterin has a prosurvival function, whereas the nuclear- and mitochondria-localized form of clusterin exhibits pro-apoptotic effects. It has been postulated that tumor cells are able to switch clusterin expression from nuclear and mitochondrial clusterin to secreted clusterin (59). Despite the conflicting reports of the role of clusterin in prostate cancer development, our study suggests that clusterin found in the plasma may serve as a useful biomarker to assess the biological effect(s) of PEITC.

Our study has some limitations. We used a transgenic mouse model of prostate cancer to demonstrate the chemopreventative

efficacy of PEITC treatment. Because mouse models do not stringently recapitulate human disease progression, the results of PEITC treatment as a chemopreventative strategy may be different in humans. It is unclear if prevention of human prostate cancer is feasible with dietary intervention with PEITC-enriched cruciferous vegetables (eg, watercress) or if a pharmacological approach with pure PEITC may be necessary for optimal activity.

Nonetheless, our study indicates that dietary PEITC administration inhibits progression to PD in TRAMP mice without any measurable side effects. We also show that PEITC-mediated inhibition of prostate cancer progression is associated with increased expression of markers of autophagy, increased expression of tumor suppressor E-cadherin, and suppression of plasma clusterin levels.

References

1. Jemal A, Siegel R, Xu J, Ward E. Cancer Statistics, 2010. *CA Cancer J Clin.* 2010;60(5):277–300.
2. Surh YJ. Cancer chemoprevention with dietary phytochemicals. *Nat Rev Cancer.* 2003;3(10):768–780.
3. Newman DJ, Cragg GM, Snader KM. Natural products as sources of new drugs over the period 1981-2002. *J Nat Prod.* 2003;66(7):1022–1037.
4. Herman-Antosiewicz A, Powolny AA, Singh SV. Molecular targets of cancer chemoprevention by garlic-derived organosulfides. *Acta Pharmacol Sin.* 2007;28(9):1355–1364.
5. Stan SD, Kar S, Stoner GD, Singh SV. Bioactive food components and cancer risk reduction. *J Cell Biochem.* 2008;104(1):339–356.
6. Stan SD, Singh SV, Brand RE. Chemoprevention strategies for pancreatic cancer. *Nat Rev Gastroenterol Hepatol.* 2010;7(6):347–356.
7. Greenwald P, Clifford CK, Milner JA. Diet and cancer prevention. *Eur J Cancer.* 2001;37(8):948–965.
8. Verhoeven DT, Goldbohm RA, van Poppel G, Verhagen H, van den Brandt PA. Epidemiological studies on brassica vegetables and cancer risk. *Cancer Epidemiol Biomarkers Prev.* 1996;5(9):733–748.
9. Kolonel LN, Hankin JH, Whittemore AS, et al. Vegetables, fruits, legumes and prostate cancer: a multiethnic case-control study. *Cancer Epidemiol Biomarkers Prev.* 2000;9(8):795–804.
10. Ambrosone CB, McCann SE, Freudenheim JL, Marshall JR, Zhang Y, Shields PG. Breast cancer risk in premenopausal women is inversely associated with consumption of broccoli, a source of isothiocyanates, but is not modified by GST genotype. *J Nutr.* 2004;134(5):1134–1138.
11. Hecht SS. Inhibition of carcinogenesis by isothiocyanates. *Drug Metab Rev.* 2000;32(3–4):395–411.
12. Fahey JW, Zalcmann AT, Talalay P. The chemical diversity and distribution of glucosinolates and isothiocyanates among plants. *Phytochemistry.* 2001;56(1):5–51.
13. Morse MA, Wang CX, Stoner GD, et al. Inhibition of 4-(methylnitrosamino)-1-(3-pyridyl)-1-butanone-induced DNA adduct formation and tumorigenicity in lung of F344 rats by dietary phenethyl isothiocyanate. *Cancer Res.* 1989;49(3):549–553.
14. Hecht SS, Trushin N, Rigotty J, et al. Complete inhibition of 4-(methylnitrosamino)-1-(3-pyridyl)-1-butanone-induced rat lung tumorigenesis and favorable modification of biomarkers by phenethyl isothiocyanate. *Cancer Epidemiol Biomarkers Prev.* 1996;5(8):645–652.
15. Pereira MA. Chemoprevention of diethylnitrosamine-induced liver foci and hepatocellular adenomas in C3H mice. *Anticancer Res.* 1995;15(5B):1953–1956.
16. Stoner GD, Morrissey DT, Heur YH, Daniel EM, Galati AJ, Wagner SA. Inhibitory effects of phenethyl isothiocyanate on N-nitrosobenzylmethylamine carcinogenesis in the rat esophagus. *Cancer Res.* 1991;51(8):2063–2068.
17. Stoner GD, Dombkowski AA, Reen RK, et al. Carcinogen-altered genes in rat esophagus positively modulated to normal levels of expression by both black raspberries and phenethyl isothiocyanate. *Cancer Res.* 2008;68(15):6460–6467.
18. Khor TO, Cheung WK, Prawan A, Reddy BS, Kong AN. Chemoprevention of familial adenomatous polyposis in Apc(Min/+) mice by phenethyl isothiocyanate (PEITC). *Mol Carcinog.* 2008;47(5):321–325.
19. Chen YR, Han J, Kori R, Kong AN, Tan TH. Phenethyl isothiocyanate induces apoptotic signaling via suppressing phosphatase activity against c-Jun N-terminal kinase. *J Biol Chem.* 2002;277(42):39334–39342.
20. Xiao D, Singh SV. Phenethyl isothiocyanate-induced apoptosis in p53-deficient PC-3 human prostate cancer cell line is mediated by extracellular signal-regulated kinases. *Cancer Res.* 2002;62(13):3615–3619.
21. Xiao D, Johnson CS, Trump DL, Singh SV. Proteasome-mediated degradation of cell division cycle 25C and cyclin-dependent kinase 1 in phenethyl isothiocyanate-induced G2-M-phase cell cycle arrest in PC-3 human prostate cancer cells. *Mol Cancer Ther.* 2004;3(5):567–575.
22. Xu C, Shen G, Chen C, Gélinas C, Kong AN. Suppression of NF-kappaB and NF-kappaB-regulated gene expression by sulforaphane and PEITC through lkappaBalpha, IKK pathway in human prostate cancer PC-3 cells. *Oncogene.* 2005;24(28):4486–4495.
23. Xiao D, Zeng Y, Choi S, Lew KL, Nelson JB, Singh SV. Caspase-dependent apoptosis induction by phenethyl isothiocyanate, a cruciferous vegetable-derived cancer chemopreventive agent, is mediated by Bak and Bax. *Clin Cancer Res.* 2005;11(7):2670–2679.
24. Xiao D, Lew KL, Zeng Y, et al. Phenethyl isothiocyanate-induced apoptosis in PC-3 human prostate cancer cells is mediated by reactive oxygen species-dependent disruption of the mitochondrial membrane potential. *Carcinogenesis.* 2006;27(11):2223–2234.
25. Bommareddy A, Hahm ER, Xiao D, et al. Atg5 regulates phenethyl isothiocyanate-induced autophagic and apoptotic cell death in human prostate cancer cells. *Cancer Res.* 2009;69(8):3704–3712.
26. Xiao D, Singh SV. p66Shc is indispensable for phenethyl isothiocyanate-induced apoptosis in human prostate cancer cells. *Cancer Res.* 2010;70(8):3150–3158.
27. Xiao D, Singh SV. Phenethyl isothiocyanate inhibits angiogenesis in vitro and ex vivo. *Cancer Res.* 2007;67(5):2239–2246.
28. Greenberg NM, DeMayo F, Finegold MJ, et al. Prostate cancer in a transgenic mouse. *Proc Natl Acad Sci U S A.* 1995;92(8):3439–3443.
29. Kaplan-Lefko PJ, Chen TM, Ittmann MM, et al. Pathobiology of autochthonous prostate cancer in a pre-clinical transgenic mouse model. *Prostate.* 2003;55(3):219–237.
30. Singh SV, Powolny AA, Stan SD, et al. Garlic constituent diallyl trisulfide prevents development of poorly differentiated prostate cancer and pulmonary metastasis multiplicity in TRAMP mice. *Cancer Res.* 2008;68(22):9503–9511.
31. Singh SV, Warin R, Xiao D, et al. Sulforaphane inhibits prostate carcinogenesis and pulmonary metastasis in TRAMP mice in association with increased cytotoxicity of natural killer cells. *Cancer Res.* 2009;69(5):2117–2125.
32. Ji Y, Kuo Y, Morris ME. Pharmacokinetics of dietary phenethyl isothiocyanate in rats. *Pharm Res.* 2005;22(10):1658–1666.
33. Foster BA, Gingrich JR, Kwon ED, Madias C, Greenberg NM. Characterization of prostatic epithelial cell lines derived from transgenic adenocarcinoma of the mouse prostate (TRAMP) model. *Cancer Res.* 1997;57(16):3325–3330.
34. Xiao D, Srivastava SK, Lew KL, et al. Allyl isothiocyanate, a constituent of cruciferous vegetables, inhibits proliferation of human prostate cancer cells by causing G_2/M arrest and inducing apoptosis. *Carcinogenesis.* 2003;24(5):891–897.
35. Xiao D, Choi S, Johnson DE, et al. Diallyl trisulfide-induced apoptosis in human prostate cancer cells involves c-Jun N-terminal kinase and extracellular-signal regulated kinase-mediated phosphorylation of Bcl-2. *Oncogene.* 2004;23(33):5594–5606.
36. Wolfinger R, O'Connell M. Generalized linear mixed models- a pseudo-likelihood approach. *J Stat Comput Simul.* 1993;48(3–4):233–243.
37. Roy-Burman P, Wu H, Powell WC, Hagenkord J, Cohen MB. Genetically defined mouse models that mimic natural aspects of human prostate cancer development. *Endocr Relat Cancer.* 2004;11(2):225–254.
38. Mucci LA, Powolny A, Giovannucci E, et al. Prospective study of prostate tumor angiogenesis and cancer-specific mortality in the health professionals follow-up study. *J Clin Oncol.* 2009;27(33):5627–5633.

39. Mathew R, Karp CM, Beaudoin B, et al. Autophagy suppresses tumorigenesis through elimination of p62. *Cell.* 2009;137(6):1062–1075.
40. Wheelock MJ, Johnson KR. Cadherins as modulators of cellular phenotype. *Annu Rev Cell Dev Biol.* 2003;19:207–235.
41. Segawa N, Mori I, Utsunomiya H, et al. Prognostic significance of neuroendocrine differentiation, proliferation activity and androgen receptor expression in prostate cancer. *Pathol Int.* 2001;51(6):452–459.
42. Aprikian AG, Cordon-Cardo C, Fair WR, et al. Neuroendocrine differentiation in metastatic prostatic adenocarcinoma. *J Urol.* 1994;151(4):914–919.
43. Greenberg JI, Cheresh DA. VEGF as an inhibitor of tumor vessel maturation: implications for cancer therapy. *Expert Opin Biol Ther.* 2009;9(11):1347–1356.
44. Miller DW, Vosseler S, Mirancea N, et al. Rapid vessel regression, protease inhibition, and stromal normalization upon short-term vascular endothelial growth factor receptor 2 inhibition in skin carcinoma heterotransplants. *Am J Pathol.* 2005;167(5):1389–1403.
45. Herman-Antosiewicz A, Johnson DE, Singh SV. Sulforaphane causes autophagy to inhibit release of cytochrome C and apoptosis in human prostate cancer cells. *Cancer Res.* 2006;66(11):5828–5835.
46. Jia L, Dourmashkin RR, Allen PD, Gray AB, Newland AC, Kelsey SM. Inhibition of autophagy abrogates tumour necrosis factor alpha induced apoptosis in human T-lymphoblastic leukaemic cells. *Br J Haematol.* 1997;98(3):673–685.
47. Bjørkøy G, Lamark T, Brech A, et al. p62/SQSTM1 forms protein aggregates degraded by autophagy and has a protective effect on huntingtin-induced cell death. *J Cell Biol.* 2005;171(4):603–614.
48. Ichimura Y, Kumanomidou T, Sou YS, et al. Structural basis for sorting mechanism of p62 in selective autophagy. *J Biol Chem.* 2008;283(33):22847–22857.
49. Komatsu M, Waguri S, Koike M, et al. Homeostatic levels of p62 control cytoplasmic inclusion body formation in autophagy-deficient mice. *Cell.* 2007;131(6):1149–1163.
50. Komatsu M, Kurokawa H, Waguri S, et al. The selective autophagy substrate p62 activates the stress responsive transcription factor Nrf2 through inactivation of Keap1. *Nat Cell Biol.* 2010;12(3):213–223.
51. Jain A, Lamark T, Sjøttem E, et al. p62/SQSTM1 is a target gene for transcription factor NRF2 and creates a positive feedback loop by inducing antioxidant response element-driven gene transcription. *J Biol Chem.* 2010;285(29):22576–22591.
52. Lau A, Wang XJ, Zhao F, et al. A noncanonical mechanism of Nrf2 activation by autophagy deficiency: direct interaction between Keap1 and p62. *Mol Cell Biol.* 2010;30(13):3275–3285.
53. Thompson HG, Harris JW, Wold BJ, Lin F, Brody JP. p62 overexpression in breast tumors and regulation by prostate-derived Ets factor in breast cancer cells. *Oncogene.* 2003;22(15):2322–2333.
54. Kitamura H, Torigoe T, Asanuma H, et al. Cytosolic overexpression of p62 sequestosome 1 in neoplastic prostate tissue. *Histopathology.* 2006;48(2):157–161.
55. Rolland P, Madjd Z, Durrant L, Ellis IO, Layfield R, Spendlove I. The ubiquitin-binding protein p62 is expressed in breast cancers showing features of aggressive disease. *Endocr Relat Cancer.* 2007;14(1):73–80.
56. Cavallaro U, Christofori G. Cell adhesion and signalling by cadherins and Ig-CAMs in cancer. *Nat Rev Cancer.* 2004;4(2):118–132.
57. Yang J, Weinberg RA. Epithelial–mesenchymal transition: at the crossroads of development and tumor metastasis. *Dev Cell.* 2008;14(6):818–829.
58. Mohammadizadeh F, Ghasemibasir H, Rajabi P, Naimi A, Eftekhari A, Mesbah A. Correlation of E-cadherin expression and routine immunohistochemistry panel in breast invasive ductal carcinoma. *Cancer Biomark.* 2009;5(1):1–8.
59. Shannan B, Seifert M, Leskov K, et al. Challenge and promise: roles for clusterin in pathogenesis, progression and therapy of cancer. *Cell Death Differ.* 2006;13(1):12–19.
60. Miyake H, Muramaki M, Kurahashi T, et al. Expression of clusterin in prostate cancer correlates with Gleason score but not with prognosis in patients undergoing radical prostatectomy without neoadjuvant hormonal therapy. *Urology.* 2006;68(3):609–614.
61. Bettuzzi S, Davalli P, Davoli S, et al. Genetic inactivation of ApoJ/clusterin: effects on prostate tumourigenesis and metastatic spread. *Oncogene.* 2009;28(49):4344–4352.

Funding

This investigation was supported in part by research grants from the National Cancer Institute at the National Institutes of Health (RO1 CA101753-07 and RO1 CA115498-05 to S.V.S., and P30-CA47904 to D.P.N., J.H.B., J.B.N., and S.V.S.).

Notes

A. A. Powolny and A. Bommareddy were responsible for randomization and feeding of mice, determination of body weights and diet consumption, collection of tissues, histopathologic evaluations, and immunohistochemical analyses. A. A. Powolny conducted electron microscopy and prepared the article. E.-R. Hahm performed immunohistochemical analysis for p62 expression and western blotting to determine the effect of various dietary compounds on clusterin expression in cell lysates and conditioned media from TRAMP-C1 cells. The levels of PEITC in plasma and prostate tissues were determined by J. H. Beumer. The statistical analyses were performed by D. P. Normolle. J. B. Nelson was involved with experimental design. S. V. Singh was responsible for the overall experimental design and supervision of the experiments, data interpretation, and preparation of the final article. The authors thank Julie A. Arlotti, Marie Acquafondata, Brian Kiesel, and Robert Parise for their technical assistance.

Affiliations of authors: Department of Pharmacology and Chemical Biology (AAP, AB, E-RH, SVS) and Department of Urology (JBN, SVS), University of Pittsburgh School of Medicine, Pittsburgh, PA; Biostatistics Department, Graduate School of Public Health, and Biostatistics Facility, University of Pittsburgh Cancer Institute, University of Pittsburgh, Pittsburgh, PA (DPN); Department of Pharmaceutical Sciences, University of Pittsburgh School of Pharmacy, Pittsburgh, PA (JHB).